Schulman, L. H., Pelka, H., & Susani, M. (1983) *Nucleic Acids Res. 11*, 1439–1455.
Seno, T., Agris, P. F., & Soll, D. (1974) *Biochim. Biophys. Acta 349*, 328–338.
Shimura, Y., Aono, H., Ozeki, H., Sarabhai, A., Lamfrom, H., & Abelson, J. (1972) *FEBS Lett. 22*, 144–148.
Silberklang, M., Gillum, A. M., & RajBhandary, U. L. (1979) *Methods Enzymol. 59*, 58–109.
Smith, J. D., & Celis, J. E. (1973) *Nature (London), New Biol. 243*, 66–71.
Steege, D. A. (1983) *Nucleic Acids Res. 11*, 3823–3832.
Thorbjarnardottir, S., Dingermann, T., Rafner, T., Andresson, O. S., Soll, D., & Eggertsson, G. (1985) *J. Bacteriol. 161*, 219–222.
Yaniv, M., & Folk, W. R. (1975) *J. Biol. Chem. 250*, 3243–3253.
Yaniv, M., Folk, W. R., Berg, P., & Soll, L. (1974) *J. Mol. Biol. 86*, 245–260.
Yarus, M. (1972) *Biochemistry 11*, 2352–2361.
Yarus, M., Knowlton, R., & Soll, L. (1977) in *Nucleic Acid-Protein Recognition* (Vogel, H., Ed.) pp 391–408, Academic Press, New York.

Glycosylation and Posttranslational Maturation of Glycoproteins in Embryonal Carcinomas: Identification of Two Distinct Pools of High-Mannose Glycans†

Raymond J. Ivatt

Department of Tumor Biology, The University of Texas M. D. Anderson Hospital and Tumor Institute at Houston, Houston, Texas 77030

Received March 14, 1985

ABSTRACT: Embryonal carcinomas and early embryonic cells assemble a family of unusually large and complex carbohydrates. These glycans contain large amounts of the sugars galactose and *N*-acetylglucosamine and are decorated with fucose, sulfate, and sialic acids. We show that, by their sensitivity to inhibition by tunicamycin and by their resistance to cleavage by alkaline hydrolysis, in teratocarcinoma stem cells the expression of these glycans is on asparagine-linked cores. These glycans are part of the large spectrum of glycans that are assembled on mannose cores derived from a common, lipid-linked precursor glycan. We examined the fate of this precursor glycan after its transfer to protein and found that there are two distinct pools of protein-linked, high-mannose glycans, which can be distinguished on the basis of their rate of processing. One pool is processed rapidly to provide a wide spectrum of complex-type glycans. This processing occurs efficiently with little evidence of intermediate structures. The other, larger pool remains unprocessed, beyond glucose removal, at a time when complex-type glycans cease to accumulate. In contrast, high-mannose glycans are relatively minor components of the glycans labeled during long-term, continuous labeling, and in this situation they are processed to provide a spectrum of trimmed glycans.

The establishment of clonal mouse teratocarcinoma stem cell lines has made available an experimental system for studying early mammalian development (Jacob, 1975; Martin, 1975, 1980; Graham, 1977; Hogan, 1977). These cells resemble the inner cell mass of the preimplantation mouse embryo, and upon aggregation and subsequent differentiation, they form a core of multipotent cells surrounded by a layer of endoderm. This pattern of differentiation closely resembles the development of the mouse inner cell mass. Changes in the expression of cell surface glycoproteins (Artzt et al., 1973; Jacob, 1977; Solter & Knowles, 1978; Ivatt, 1984) and the progressive reduction of agglutinability of the mouse embryo by lectins during development (Magnuson & Stackpole, 1978; Magnuson & Epstein, 1981) have implicated cell surface carbohydrates as being functionally involved. This attitude is reinforced by the observation that inhibition of protein glycosylation by tunicamycin inhibits blastocyst compaction and trophoblast adhesion (Surani, 1979).

The focus of this investigation is the assembly of an unusual class of glycans that appears to be characteristic of early embryonic cells and that is expressed by embryonal carcinomas. These glycans are very large and are reported to be rich in galactose and *N*-acetylglucosamine (Muramatsu et al., 1980). These glycans are termed poly(lactosamines) and share many properties with erythroglycans, poly(lactosamines) expressed by red blood cells (Finne et al., 1978; Jarnefelt et al., 1978; Fukuda et al., 1979). These large embryonic glycans were originally identified from cultures metabolically labeled with fucose. They showed a dramatic decrease during both normal embryonic development and after extensive differentiation by embryonal carcinoma cultures (Muramatsu et al., 1978).

We investigated the assembly of glycoprotein determinants in embryonal carcinomas. Using tunicamycin inhibition and chemical sensitivity as criteria, we show that, in teratocarcinoma cells, the unusually large carbohydrate units are attached to asparagine residues. Asparagine-linked glycans have been demonstrated in fibroblastic cells to be assembled on mannose

† This investigation was supported by Grants CD-153 and BC-426 from the American Cancer Society and by Grant G-891 from the Robert A. Welch Foundation. R.J.I. is the recipient of March of Dimes Birth Defects Foundation–Basil O'Connor Starter Research Grant MOD 5-365.

0006-2960/85/0424-7314$01.50/0 © 1985 American Chemical Society

cores as products of a long and complex biosynthetic pathway (Elbein, 1979; Parodi & Leloir, 1979; Spiro & Spiro, 1979; Kornfeld & Kornfeld, 1980; Struck & Lennarz, 1980; Hubbard & Ivatt, 1981). These glycan products are the result of competition between rival glycosylation pathways for a common acceptor glycan derived by extensive trimming from the lipid-linked precursor glycan (Paulson et al., 1978; Beyer et al., 1981; Ivatt, 1981). We have identified a lipid-linked precursor glycan in teratocarcinoma stem cells that is identical in its properties with the one described for fibroblastic cells, and we have studied its metabolism. Our examination of the fate of the glycan after its transfer to protein has identified two distinct pools of high-mannose precursor glycans.

Materials and Methods

Materials. Endo-β-*N*-acetylglucosaminidase H (endo-H) was prepared from *Streptomyces plicatus* according to the method of Tarentino et al. (1978). α-Mannosidase type III and neuraminidase type X were obtained from Sigma Chemical Co., St. Louis, MO. Bio-Gel P-4 and Bio-Gel P-10 were obtained from Bio-Rad Laboratories, Richmond, CA, and Pronase CB was obtained from Calbiochem, San Diego, CA. The radiochemicals were from New England Nuclear, Boston, MA (D-[2-^{3}H(N)]Man, 10–20 Ci/mmol).

Culture Conditions. F9 murine teratocarcinoma cells were maintained as described by Martin (1975).

Cell Labeling. For the pulse and pulse/chase experiments, the F9 cells were washed with glucose (Glc) free medium 3 times and then were metabolically labeled with mannose (Man), 1 mCi/mL, in Glc-free medium. Pulse lengths varied from $2^1/_2$ to 40 min and are described in the text. For the times described in the text, chases were performed in complete medium with 5% fetal calf serum after three washes with complete medium.

Preparation of Lipid-Linked and Protein-Linked Oligosaccharides. The cells were subjected to a modified Folch extraction (Folch et al., 1957) as described previously (Ivatt et al., 1984). The interface and lower phase were adjusted to construct a single phase of chloroform/methanol/water (10:10:3). The pellet formed by centrifugation provided the protein-linked oligosaccharides while the chloroform/methanol/water (10:10:3) washes provided the lipid-linked oligosaccharide. The lipid-linked oligosaccharide was released by mild acid hydrolysis performed in 50 mM trifluoroacetic acid and 20% isopropanol, for 20 min at 100 °C. Glycopeptides were prepared by sequential digestions with Pronase and endo-H as described previously (Ivatt et al., 1984).

Glycohydrolase Digestions. Sensitivity to endo-H was tested in 0.1 M citrate, pH 5.5, with 90 milliunits of enzyme at 37 °C for 4 h under a toluene atmosphere. Exhaustive α-mannosidase digestion was performed as described by Liu et al. (1979).

Acetolysis. Endo-H-treated glycans were reduced with sodium borohydride and subjected to acetolysis as described by Tai et al. (1975).

Chromatographic Techniques. Gel filtration was performed either on columns (1.3 × 90 cm) of Bio-Gel P-4 (minus 400 mesh) or on mixed-bed columns (1.3 × 100 cm) of Bio-Gel P-4 (upper 60 cm of column packing) and Bio-Gel P-10 (lower 30 cm of column packing). Both materials were minus 400 mesh. The mixed-bed columns are referred to as Bio-Gel P-4/P-10 columns. Columns were eluted with 50 mM pyridinium acetate, pH 5.5, containing 0.05% NaN_3, at a flow rate of 4.0 mL/h. Fractions of 0.45 mL were collected. Descending paper chromatography was performed on Whatman No. 1 paper in the following solvent systems: solvent A, pyridine/ethyl acetate/acetic acid/water (5:5:1:3); solvent B, pyridine/ethyl acetate/water (1:3.6:1.14), upper phase.

Sodium Dodecyl Sulfate–Polyacrylamide Gel Electrophoresis (SDS–PAGE)/Fluorography. Metabolically labeled F9 cells were washed with desalting buffer [10 mM tris(hydroxymethyl)aminomethane hydrochloride (Tris-HCl), pH 7.2, 0.25 M sucrose, 0.05 mM $CaCl_2$, 10 μM phenylmethanesulfonyl fluoride (PMSF)] and solubilized with 500 μL of the same containing 0.5% Nonidet P-40 (NP-40). The cell extracts were centrifuged, 250 μL of 3× SDS–PAGE sample buffer [186 mM Tris–PO_4, pH 6.7, 6% SDS, 1.5 mM ethylenediaminetetraacetic acid (EDTA), 10% glycerol, 100 mM dithiothreitol, 0.003% bromophenol blue] was added to the supernatant, and the samples were heated for 5 min at 100 °C before being applied to the polyacrylamide gel. The gel consisted of a 10% slab (3.0-mm) and 5% stacking gel. The discontinuous SDS buffering system of Laemmli (1970) was used with a Tris–PO_4 stacking gel and the sample buffer of Maizel (1971). The gel was run at 5 W (constant power) for stacking and at 30 W for the running gel. The gel was fixed for 1 h in 10% trichloroacetic acid (TCA), 10% acetic acid, and 30% isopropanol, treated with Enhance (New England Nuclear), and dried, and Kodak XAR-5 film exposed to it at −70 °C for 2 days.

Results

Glycoprotein-Linked Glycans Assembled by Teratocarcinoma Stem Cells. The complex glycans found on mature glycoproteins of teratocarcinoma cells are much larger than are the comparable glycans assembled by fibroblastic cells (Muramatsu et al., 1978).

The complex-type glycans that are found on mature glycoproteins of fibroblasts are the products of a long and complex pathway that involves extensive trimming of a precursor glycan and reassembly on this processed core. This processing is not always completed, and therefore, a spectrum of glycoprotein-linked glycans is expressed, ranging from the precursor glycan to the many lactosamine-containing glycans that are the late products of this pathway. Two approaches were followed to determine what proportion of the unusually large glycans were asparagine-linked. The sensitivity of the glycan–protein linkage to mild alkaline digestion was examined, and also the sensitivity of the assembly of these glycans to inhibition by the drug tunicamycin was examined (Figure 1).

There is very little metabolically labeled carbohydrate released from the stem cell glycoproteins after 48 h of mild alkaline hydrolysis, either galactose (Gal), glucosamine ($GlcNH_2$), or fucose (Fuc) labeling (Figure 1A, right panel). This is a condition that almost completely depolymerizes glycophorin-like glycopeptides from human K-562 erythroleukemic cells (Figure 1A, left panel, screwheads). The small amount of material released from F9 glycoproteins is actually comparable to the amount released from glycoproteins prepared from cells that have been pulse-labeled with Man under conditions which ensure that only high-Man precursor glycans are present (Figure 1A, left panel, open symbols). (These endo-H-sensitive glycans are the best marker we have for asparagine-linked glycans.) Therefore, the low level of glycan released on mild alkaline hydrolysis is much more likely to be the result of cleavage of peptide–peptide linkages than of glycan–peptide linkages.

At intermediate concentrations, the incorporation of Man into glycoproteins is much more sensitive to inhibition by tunicamycin than is the incorporation of leucine (Figure 1B). At 10 μg/mL, the cells detach from the plates and have a low level of incorporation of both leucine and Man, and at less than

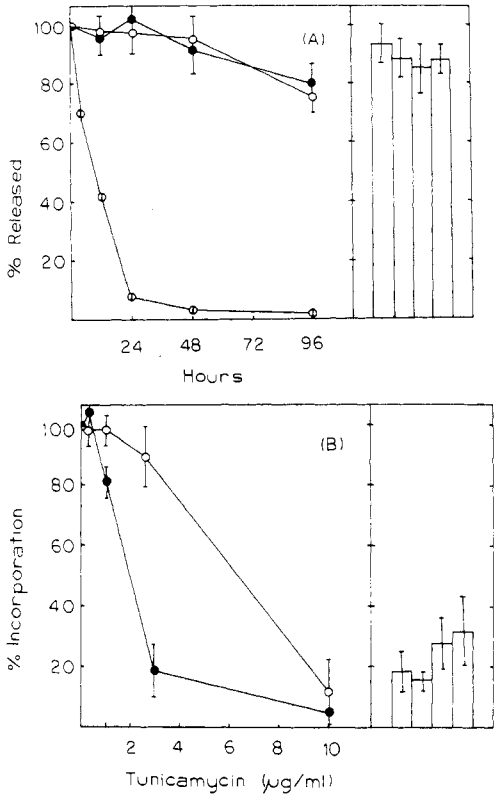

FIGURE 1: Nature of the linkage to protein. (A) Resistance of protein-linked glycans to release by mild reductive alkaline conditions. The left panel shows the rapid hydrolysis of glycophorin-like glycopeptides prepared from human K-562 erythroleukemic cells (screwheads) and the slow release of Fuc (solid symbols) and Man (open symbols) from metabolically labeled F9 glycoproteins into the TCA-soluble pool. F9 cells were labeled with Fuc overnight or with Man for 15 min. The cells were then exhaustively extracted with solvents to remove glycolipids and unincorporated sugars and then incubated in alkaline conditions. Aliquots were removed after various times, and the material still insoluble in TCA was measured. The right panel compares the proportion of, from left to right, Man-, Fuc-, Gal-, and $GlcNH_2$-labeled material still insoluble in TCA after 48 h of hydrolysis. (B) Effect of tunicamycin upon the incorporation of metabolic labels. The left panel shows the differential inhibition of Man (solid symbols) and leucine (open symbols) incorporations at intermediate concentrations of tunicamycin. The right panel shows the coordinated inhibition of, from left to right, Man, Fuc, Gal, and $GlcNH_2$ at 3 μg/mL tunicamycin. Cells were preincubated with tunicamycin for 18 h and then incubated with radiolabeled precursors for 6 h. The incorporation represents the residual label not extracted as glycolipid or unincorporated precursor.

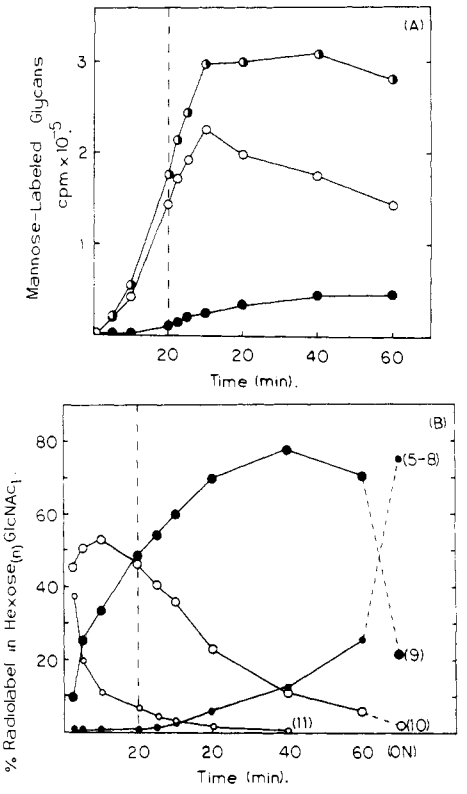

FIGURE 2: (A) Analysis of the protein-linked glycans as a function of increasing pulse length with [^{3}H]Man and as a function of increasing chase length following a 20-min pulse label (vertical dashed line). The amount of radiolabel in endo-H-resistant (solid symbols) and endo-H-sensitive (open symbols) glycans is shown. The halved symbols represent the total level of protein-linked glycans calculated on the basis of three Man residues per endo-H-resistant glycan and nine Man residues per endo-H-sensitive glycan and provide an estimate of glycoprotein turnover. (B) Size distribution of the endo-H-sensitive, protein-linked glycans as a function of increasing pulse length with [^{3}H]Man and as a function of increasing chase length following a 20-min pulse (vertical dashed line). The proportion of protein-linked radiolabel in a particular species is plotted against time. The number of hexose units attached to GlcNAc (in parentheses) identifies the size of the glycan. The symbols connected by dashes are the values for these species in the protein-linked glycans prepared from cells that have been labeled continuously with [^{3}H]Man for 18 h.

1 μg/mL, the cells are apparently unaffected by the drug. The observation that 3 μg/mL tunicamycin similarly inhibits the incorporation of Fuc, $GlcNH_2$, Gal, and Man into the high-molecular-weight fraction suggests that the former sugars are added to Man cores derived from the lipid-linked precursor glycan. The chemical stability of these glycans and the drug sensitivity of their assembly identify the stem cell glycans as being asparagine-linked.

Formation of a Lipid-Linked Precursor Glycan and Its Transfer to Protein. Complex-type oligosaccharides are not evident after short periods of exposure to radiolabeled Man. For example, after a 15-min exposure to [^{3}H]Man, 98% of the protein-linked glycans are still sensitive to endo-H, and these glycans are two and three hexose residues smaller than the lipid-linked precursor glycan. The lipid-linked glycan behaves as 12 hexose residues attached to *N*-acetylglucosamine (GlcNAc) and is always the major species during pulse and pulse/chase experiments. The kinetics of its assembly and turnover are very similar to those previously described for fibroblastic cells [e.g., Hubbard & Robbins (1979, 1980)].

Fate of the High-Man Glycans after Transfer to Protein. The glycans transferred to protein are exclusively of the high-Man type, and with increasing chase time endo-H-resistant glycans accumulate. The time courses for the appearance of complex-type glycans and the disappearance of high-Man glycans are shown in Figure 2A. The profiles show the sensitivity of the glycans to endo-H as a function of time after a pulse-labeling period. After the 10-min pulse-labeling period, there is very little material resistant to endo-H, but during more extensive pulse-labeling periods and during chase periods following a pulse, the proportion of endo-H-resistant material increases. The Man label disappears from the high-Man structures faster than it appears in the complex-type structures, consistent with the common observation that complex-type glycans have three Man residues in their core and high-Man structures have a complement of nine Man residues.

The glycans initially transferred to protein are similar in size to the lipid-linked precursor glycan. However, with time, the proportion of glycan chains with this close size correspondence decreases (Figure 2B). The first and second hexose (Hex) residues are removed very rapidly after the transfer of the precursor glycan to protein. The third hexose residue is removed much more slowly. Protein-linked glycans with the

same size as the precursor glycan are barely detectable even when the pulse is as short as $2^1/_2$ min. Almost half of the glycans at this stage have lost two hexose residues. However, after a $2^1/_2$-min chase following a 20-min pulse only half of the glycans have lost more than two hexose residues, and there are no detectable glycans that have lost more than three hexoses (Figure 2B). Glycans that elute as $Hex_9GlcNAc$ are extensively degraded during exhaustive α-mannosidase digestion and release 88% of the label as free Man and 12% of the label as a glycan that comigrates with $Man_1GlcNAc$. In contrast, glycans that elute as $Hex_{10}GlcNAc$ release only 45% of the label as free Man, and 55% of the label is retained as glycans that migrate as $Hex_6GlcNAc_2$ (45%) and $Hex_7GlcNAc_2$ (10%). The bulk (80%) of the high-Man structures present after a 60-min chase following a 20-min pulse still contain nine Man residues. Therefore, at this time, there has been little apparent trimming of the precursor glycan beyond the removal of the first three hexose (Glc) residues, although at this time there has been extensive conversion to complex-type glycans and the level of these glycan has stabilized (Figure 2A).

In contrast, the endo-H-sensitive glycans prepared from glycoproteins labeled during a long, continuous label demonstrate extensive trimming with less than 20% of the glycans retaining nine Man residues (symbols connected by dashed lines, Figure 2B). There are, therefore, two distinct classes of high-Man glycans—those that are trimmed and converted to complex-type glycans with little evidence of intermediate forms and those that appear to be more resistant to extensive trimming.

Slow Processing of High-Man Glycans Is Not the Result of Abnormalities in Lipid-Linked Precursor Glycan. The difference in the proportion and size distribution of the high-Man glycans, from long, continuously labeled and pulse-labeled cells, could, in principle, be the result of the different labeling protocols. Therefore, it was important to establish that the glucose-free labeling conditions utilized during short pulse labelings were not responsible for abnormalities in the synthesis or transfer of the lipid-linked glycan.

Glucose deprivation does not have immediate effects upon the shape of the lipid-linked glycan profiles. Cells were pulse-labeled with Man for 5 min after increasing preincubation with Glc-free medium. Up to 20 min of preincubation has little effect upon either the size distribution (Figure 3A) or total incorporation. Even a 40-min preincubation results in slight increases in $Man_5GlcNAc_2$ (12% of total, up from 9%) and in the amount of radiolabel incorporated (up by about 20%). The $Man_5GlcNAc_2$ formed after 40 min of preincubation is resistant to endo-H digestion, and upon exhaustive α-mannosidase digestion, yields 4 mol of free Man and 1 mol of a product that comigrates with $Man_1GlcNAc_2$. The lipid-linked glycans formed at this stage that elute as $Hex_8GlcNAc_2$ are also sensitive to α-mannosidase. There is no evidence for early glycosylation of $Man_5GlcNAc_2$ as reported in Chinese hamster ovary cells (Chapman et al., 1979).

The absence of abnormally formed lipid-linked glycans is also suggested by the following kinetic analyses. During a chase period, there is a lag before the level of radioactive Man decreases from the lipid-linked pool. The rate at which the radiolabel disappears during the chase period (open symbols, Figure 3B) follows similar kinetics to the rate of entry during the pulse periods (solid symbols, Figure 3B). The rate of appearance of radiolabel into the protein-linked material remains stable during the fist few minutes of a chase period and then decreases. At all times during pulse and chase periods,

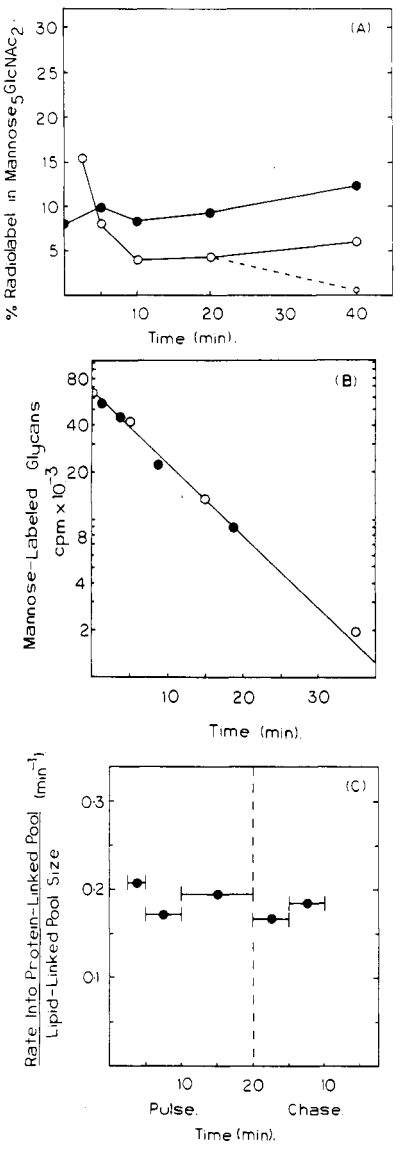

FIGURE 3: Proportion of radiolabel in the lipid-linked glycan pool that is in $Man_5GlcNAc_2$ and kinetic analyses of the turnover of the lipid-linked pool. (A) The open symbols represent the proportion of radiolabel in this species as a function of increasing pulse length with [^{3}H]Man. The small, open circle connected by a dashed line represents the proportion of this species present when a 20-min chase follows a 20-min pulse label. The solid symbols represent the proportion of radiolabel in this species when cells are pulse-labeled for 5 min following different periods of preincubation in Glc-free medium. (B) The amount of radiolabel present in the lipid-linked glycan pool is plotted as a function of time during increasing pulse lengths with [^{3}H]Man (solid symbols) and increasing chase lengths following a 20-min pulse label (open symbols). (C) The rate of incorporation of radiolabel into the protein-linked glycan pool as a function of the lipid-linked pool size after different pulse lengths with [^{3}H]Man and after different chase lengths following a 20-min pulse label is shown.

the rate of entry into the protein-linked pool reflects the total level of radiolabel in the lipid-linked pool. These simialr rates of turnover suggest that equivalent lipid-linked glycan species are present at early and late stages during the pulse labeling and that abnormally formed species, if they occur at all, are minor components. This is emphasized by the data in Figure 3C where the rate of incorporation into protein-linked glycans is correlated with lipid-linked pool size during the pulse and chase periods. The points fall close to a value of 1.8 cpm/min transferred to protein per 10 cpm in the lipid-linked pool. This value, based upon *both* the rate of appearance of label into the protein-linked pool *and* the size of the radiolabeled lipid-

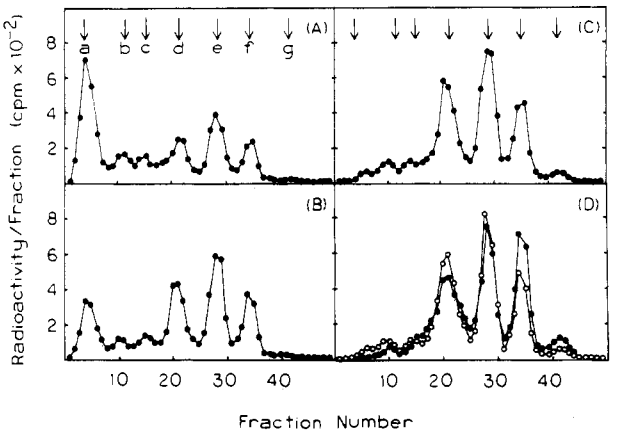

FIGURE 4: Comparison of the fragments produced by acetolysis of the protein-linked $Man_9GlcNAc$ isolated from F9 cells metabolically labeled either for 20 min or for 20 min with a subsequent 60-min chase. Endo-H-sensitive glycans were prepared as described previously, and the species corresponding to $Man_9GlcNAc$ were pooled, reduced, and subjected to acetolysis as described under Materials and Methods. The fragments produced from pulse-labeled $Man_9GlcNAc$ after (A) 3, (B) 6, (C) 12, and (D) 18 h of acetolysis are shown by the solid symbols. The corresponding fragments produced after 12 h of hydrolysis of $Man_9GlcNAc$ prepared from pulse/chased cells are shown by the open symbols in panel D. The arrows correspond to the elution positions on paper chromatography: (a–d) Man_9-, Man_7-, Man_6-, and $Man_4GlcNAc$; (e–g) Man_3, Man_2, and Man.

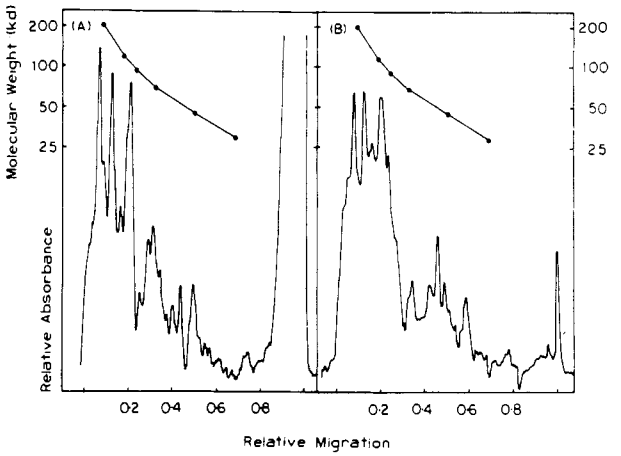

FIGURE 5: Metabolically labeled proteins prepared from F9 cells under labeling conditions where the protein-linked glycans are either exclusively high-Man or predominantly complex. F9 cells were labeled either for 15 min (A) or for 18 h (B) with Man, and the glycoproteins were extracted and analyzed by electrophoresis on SDS–PAGE. The profiles represent densitometric traces of the fluorograms. The solid symbols at the top correspond to the migration of standard proteins with the following molecular weights: 205K, 116K, 97K, 66K, 45K, and 29K. The large peak that coelutes with the dye front is the lipid-linked precursor glycan.

linked glycan pool, yields a turnover rate very similar to the one calculated *solely* from the rate of change of label in the lipid-linked pool. This finding shows that abnormalities in transfer of this glycan to protein, such as direct hydrolysis or slow transfer of an abnormal glycan, do not increase with increasing pulse length.

While the transfer of glycans based on the (endo-H-resistant) $Man_5GlcNAc_2$ core occurs at a very low frequency, the transfer of an endo-H-sensitive but abnormal glycan could not be eliminated. We therefore compared the structures of the endo-H-sensitive, protein-linked glycans present after a short pulse or after a chase period when endo-H-resistant glycans have ceased to accumulate. Acetolysis is a very valuable approach for the analysis of these endo-H-sensitive glycans, with 1–6 linkages being preferentially cleaved. However, significant cleavage of other linkages occurs before complete hydrolysis of 1–6 linkages, and comparison of the acetolysis products formed during a time course therefore provides a great deal of information regarding the similarity of two structures. The size distributions of the acetolysis products formed from the $Man_9GlcNAc$ glycans present after a short pulse are shown in Figure 4. The $Man_9GlcNAc$ starting material is lost very rapidly and is replaced by a series of smaller glycans. Fragments that comigrate with Man_3 and Man_2 oligomers accumulate. In addition, there are a series of fragments that are larger than these oligomers. These fragments show a gradual reduction in average size. Material that elutes at fraction 21 accumulates and is sensitive to α-mannosidase digestion, releasing free Man and a disaccharide that coelutes with ManGlcNAc on both paper chromatogrpahy (where the contributions of Man and GlcNAc are equivalent) and gel filtration (where the contribution of GlcNAc is equivalent to that of about three Man). Upon prolonged acetolysis, the Man_3 oligomer decreases while free Man accumulates. The pattern of fragments produced from the Man_9 glycans present after a 60-min chase is very similar (compare open symbols, Figure 4D, with solid symbols, Figure 4C).

. *Slowly Processed High-Man Glycans Are Not on Different Glycoproteins.* The two pools of high-Man glycans that are processed with different rates could, in principle, be on different carrier proteins. The experiments described in Figure 5 suggest that this is not the case. F9 cells were metabolically labeled with Man either during a 15-min pulse or during a long, continuous pulse. The short pulse provides glycoproteins that carry glycans that are exclusively high Man in character. In contrast, the long, continuous label provides glycoproteins that carry glycans that are predominantly complex in nature. When the glycoproteins labeled by these different protocols are examined by SDS–PAGE, the major labeled proteins have very similar molecular weight distributions. In both cases, the bulk of the label is incorporated into proteins that are apparently larger than 100 kilodaltons (kDa) but smaller than 250 kDa. The major peaks obtained during the long, continuous label are slightly larger than the corresponding peaks obtained during the short pulse as would be predicted from the increase in molecular weight of the carbohydrate during glycoprotein maturation.

The cellular location of the glycoproteins labeled during a long, continuous pulse and during a short pulse has been investigated using the accessibility of the metabolically labeled glycoproteins to trypsin. F9 cells were labeled with Man either for 15 min or for 18 h and then digested with trypsin in the absence of calcium. The cells were pelleted, and the material released by trypsin digestion was then exhaustively digested with Pronase while the cell pellet was Folch-extracted and the cellular material was processed as described above. The Pronase-treated glycopeptides were then digested with endo-H and examined by gel filtration on columns of Bio-Gel P-10/P-4. Very little incorporated radiolabel (less than 5%) is released by trypsin treatment of cells labeled during a short pulse. In contrast, the bulk (about 80%) of the incorporated radiolabel is released from cells trypsinized after a long, continuous label. The glycopeptides released by trypsin from cells labeled during the long label are predominantly endo-H-resistant, while glycopeptides retained by pulse-labeled cells after trypsin treatment are predominantly endo-H-sensitive. Cells that had been pulse-labeled for 20 min and then chased for 60 min were also digested with trypsin under similar conditions, and the released and retained glycans were analyzed. The material retained by the cells was predominantly

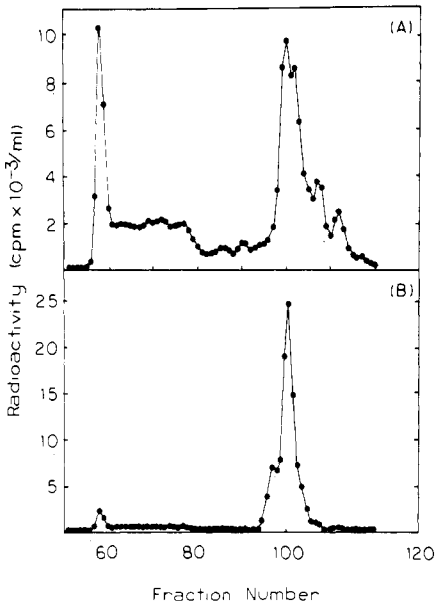

FIGURE 6: Size distribution of the protein-linked glycans prepared from (A) trypsin-sensitive and (B) trypsin-resistant compartments of cells chased for 60 min after a 20-min pulse label with Man. The cells were trypsinized as described under Materials and Methods and then centrifuged. The material remaining in the supernatant after trypsinization (A) and the material sedimenting with the cells (B) were separately pooled. The supernatant material was exhaustively digested with Pronase, the cell pellets were Folch-extracted, and the glycopeptides were prepared as described previously. The protein-linked glycans, after endo-H digestion, were analyzed by gel filtration on Bio-Gel P-4 columns.

endo-H-sensitive and mostly unprocessed $Man_9GlcNAc$ (Figure 6B). In contrast, the material released from these cells was predominantly endo-H-resistant (Figure 6A) and very similar in size distribution to the material released from cells labeled during a long, continuous label. The cellular locations of corresponding glycans labeled under these different labeling conditions are equivalent, with the bulk of the complex-type glycans on glycoproteins accessible to trypsin and the bulk of the glycans inaccessible to trypsin having a high-Man character.

Discussion

In this study, we demonstrate that a class of unusual glycans prevalent on the surfaces of both early embryonic and embryonal carcinoma cells is in the latter assembled as asparagine-linked glycans. Asparagine-linked glycans are a heterogeneous group of compounds derived from a common precursor glycan. We examined the processing of the precursor glycan in teratocarcinoma cells and found it to be similar to the pathway recently established for fibroblastic cells. The Man core is assembled on a carrier lipid as part of a much larger glycan and is transferred en bloc to protein acceptors. Overall, the kinetics of these various steps are very similar to those reported for NIL-8 fibroblastic cells (Hubbard & Robbins, 1979, 1980). Some of these precursor glycan chains are trimmed rapidly during the maturation of the glycoproteins to expose a core strucure. The glycans assembled on this core structure are very heterogeneous in size and include an unusual class of glycans that contain repeating lactosamine units [poly(lactosamine) glycans].

During the conversion of the high-Man protein-linked glycans to complex-type glycans, there are two discernible classes of high-Man glycan. One class is rapidly and extensively trimmed to form the core structure with little evidence of intermediate structures. The other class is hardly trimmed at all beyond the removal of three hexose (glucose) residues. The very low steady-state level of partially trimmed glycans during this conversion suggests that the reactions involved in processing are very efficiently coordinated and that once processing of a glycan chain begins, it rapidly goes to completion. In contrast, the second class of high-Man glycans is processed very slowly. These two classes of high-Man glycans appear to be structurally identical and to be on similar spectra of protein carriers.

Acknowledgments

The excellent technical assistance of John Reeder and Zahra Mansouri is gratefully acknowledged.

References

Artzt, K., Dubois, P., Bennett, D., Condamine, H., Babinet, C., & Jacob, F. (1973) *Proc. Natl. Acad. Sci. U.S.A. 70*, 2988–2992.

Beyer, T. A., Sadler, J. E., Rearick, J. I., Paulson, J. C., & Hill, R. L. (1981) *Adv. Enzymol. Relat. Areas Mol. Biol. 52*, 23–176.

Chapman, A., Li, E., & Kornfeld, S. (1979) *J. Biol. Chem. 254*, 10243–10249.

Elbein, A. D. (1979) *Annu. Rev. Plant Physiol. 30*, 239–272.

Finne, J., Krusius, T., Rauvala, H., Kekomaki, R., & Myllyla, G. (1978) *FEBS Lett. 89*, 111–114.

Folch, J., Lees, M., & Sloane-Starkey, G. H. (1957) *J. Biol. Chem. 226*, 497–502.

Fukuda, M., Fukuda, M. N., & Hakomori, S. I. (1979) *J. Biol. Chem. 254*, 3700–3703.

Graham, C. F. (1977) in *Concepts in Mammalian Embryogenesis* (Sherman, M. I., Ed.) pp 315–376, MIT Press, Cambridge, MA.

Hogan, B. L. M. (1977) in *Biochemistry of Cell Differentiation* (Paul, J., Ed.) pp 333–376, University Park Press, Baltimore.

Hubbard, S. C., & Robbins, P. W. (1979) *J. Biol. Chem. 254*, 4568–4576.

Hubbard, S. C., & Robbins, P. W. (1980) *J. Biol. Chem. 255*, 11782–11793.

Hubbard, S. C., & Ivatt, R. J. (1981) *Annu. Rev. Biochem. 50*, 555–583.

Ivatt, R. J. (1981) *Proc. Natl. Acad. Sci. U.S.A. 78*, 4021–4025.

Ivatt, R. J. (1984) in *The Biology of Glycoproteins* (Ivatt, R. J., Ed.) pp 95–181, Plenum Press, New York.

Ivatt, R. J., Das, O. P., Henderson, E. J., & Robbins, P. W. (1984) *Cell (Cambridge, Mass.) 38*, 561–567.

Jacob, F. (1975) *Symp. Br. Soc. Dev. Biol., 2nd*, 233–241.

Jacob, F. (1977) *Immunol. Rev. 33*, 3–32.

Jarnefelt, J., Rush, J., Li, Y. T., & Laine, R. A. (1978) *J. Biol. Chem. 253*, 8006–8009.

Kornfeld, R., & Kornfeld, S. (1980) in *The Biochemistry of Glycoproteins and Proteoglycans* (Lennarz, W. J., Ed.) pp 1–34, Plenum Press, New York.

Laemmli, U. K. (1970) *Nature (London) 227*, 680–685.

Liu, T., Stetson, B., Turco, S. J., Hubbard, S. C., & Robbins, P. W. (1979) *J. Biol. Chem. 254*, 4554–4559.

Magnuson, T., & Stackpole, C. W. (1978) *Exp. Cell Res. 116*, 466–469.

Magnuson, T., & Epstein, C. J. (1981) *Dev. Biol. 81*, 193–199.

Maizel, J. V., Jr. (1971) *Methods Virol. 5*, 179.

Martin, G. R. (1975) *Cell (Cambridge, Mass.) 5*, 229–243.

Martin, G. R. (1980) *Science (Washington, D.C.) 209*, 768–776.

Muramatsu, T., Gachelin, G., Nicolas, J. F., Condamine, H., Jakob, H., & Jacob, F. (1978) *Proc. Natl. Acad. Sci. U.S.A. 75*, 2315–2319.
Muramatsu, T., Condamine, H., Gachelin, G., & Jacob, F. (1980) *J. Embryol. Exp. Morphol. 57*, 25–36.
Parodi, A. J., & Leloir, L. F. (1979) *Biochim. Biophys. Acta 559*, 1–37.
Paulson, J. C., Priels, J. P., Glasgow, L. R., & Hill, R. L. (1978) *J. Biol. Chem. 253*, 5617–5624.
Solter, D., & Knowles, B. B. (1978) *Proc. Natl. Acad. Sci. U.S.A. 75*, 5565–5569.
Spiro, R. G., & Spiro, M. J. (1979) in *Glycoconjugate Research* (Gregory, J., & Jeanloz, R., Ed.) Vol. 2, pp 613–636, Academic Press, New York.
Struck, D. K., & Lennarz, W. J. (1980) in *The Biochemistry of Glycoproteins and Proteoglycans* (Lennarz, W. J., Ed.) pp 25–84, Plenum Press, New York.
Surani, M. A. H. (1979) *Cell (Cambridge, Mass.) 18*, 217–227.
Tai, T., Yamashita, K., Ogata-Arakaw, M., Koide, N., Muramatsu, T., Iwashita, S., Inoue, Y., & Kobata, A. (1975) *J. Biol. Chem. 250*, 8569–8575.
Tarentino, A. L., Trimble, R., & Maley, F. (1978) *Methods Enzymol. 50*, 574–579.

Purification of Nuclear and Mitochondrial Uracil–DNA Glycosylase from Rat Liver. Identification of Two Distinct Subcellular Forms†

John D. Domena‡ and Dale W. Mosbaugh*

Clayton Foundation Biochemical Institute and Department of Chemistry, The University of Texas at Austin, Austin, Texas 78712

Received February 25, 1985; Revised Manuscript Received June 13, 1985

ABSTRACT: Rat liver uracil–DNA glycosylase has been purified from nuclear extracts over 3000-fold to apparent homogeneity as determined by sodium dodecyl sulfate–polyacrylamide gel electrophoresis. The enzyme is a monomeric protein with a polypeptide molecular weight of approximately 35 000. It has a native molecular weight of 33 000 as determined by gel filtration chromatography and a sedimentation coefficient of 2.6 S in glycerol gradients. The nuclear enzyme has an alkaline pH optimum and a p*I* value of 9.3. Nuclear uracil–DNA glycosylase catalyzes the release of free uracil from both single-stranded and double-stranded DNA with the former being the preferred substrate. The enzyme is unable to recognize dUTP, dUMP, or poly(dA-dT) containing a 3′-terminal uracil residue as a substrate. However, internalization of terminal uracil residues by limited chain elongation produced a substrate for the glycosylase. Another species of uracil–DNA glycosylase has been partially purified from mitochondria. This activity differs from the nuclear enzyme in that it has (i) distinctive chromatographic properties, (ii) a lower native molecular weight of 20 000 as determined by molecular sieving, (iii) a distinct NaCl inhibition profile, and (iv) a longer half-life during thermal denaturation.

Uracil residues can be introduced into DNA during DNA synthesis or by chemical modification of existing cytosine in DNA. The incorporation of deoxyuridine monophosphate into DNA occurs efficiently by DNA polymerases, since no significant difference exists between the K_m values for dUTP and dTTP (Shlomai & Kornberg, 1978; Dube et al., 1979). Thus, dUMP incorporation, in place of dTMP, into nascent DNA is primarily dependent on the relative intracellular concentration of the two deoxyribonucleoside triphosphates. Under normal physiological conditions, the dUTP to dTTP ratio in mammalian cells is less than $1/10^5$ (Goulian et al., 1980a). Intracellular dUTP is normally limited by the action of deoxyuridinetriphosphatase which rapidly hydrolyzes dUTP to dUMP and PP_i (Williams & Cheng, 1979; Ingraham & Goulian, 1982). However, perturbations that increase the cellular dUTP/dTTP ratio result in increased incorporation of dUMP into DNA which contributes to cytotoxic effects (Goulian et al., 1980a). Uracil may also arise in nonreplicating DNA upon deamination of cytosine residues by hydrolytic reactions (Lindahl & Nyberg, 1974) or by mutagenic agents (Shapiro & Pohl, 1968; Shapiro et al., 1973). On the basis of the rate of spontaneous cytosine deamination of duplex DNA, the extent of uracil formed per genome during each mammalian cell generation could account for the conversion of at least 150 cytosine to uracil residues. However, the extent of cytosine deamination may actually be significantly higher since cytosine in single-stranded DNA deaminates at a rate 200–300 times faster than that in a double-stranded polymer (Lindahl, 1979). Deamination of cytosine in duplex DNA forms G·U mismatched base pairs which are premutagenic lesions. If such uracil residues remain in the genome during DNA replication, G·C → A·T transition mutations will occur (Duncan & Miller, 1980). Fortunately, uracil residues are normally introduced only as transient components of prokaryotic and eukaryotic DNA (Tye et al., 1977; Goulian et al., 1980b).

Uracil–DNA glycosylases catalyze the removal of uracil from DNA by cleaving the N-glycosylic bond between uracil and deoxyribose (Lindahl et al., 1977; Lindahl, 1982). This process leaves an apyrimidinic site in the phosphodiester chain

† This work was supported by Grant GM32823 from the National Institutes of Health.
* Address correspondence to this author at the Department of Chemistry, The University of Texas at Austin.
‡ Recipient of Predoctoral Traineeship T32-CA09182 from the National Institutes of Health in support of this work.

0006-2960/85/0424-7320$01.50/0 © 1985 American Chemical Society